SUPPORTING INFORMATION

A ROS Scavenging Protein Nanocage for *In Vitro* and *In Vivo* Antioxidant Treatment

*Weiwei Zhu[a,c†], Ti Fang[a†], Wenjing Zhang[a,c], Ao Liang[a,c], Hui Zhang[a], Zhi-Ping Zhang[a], Xian-En Zhang[b,c] and Feng Li[a,c]**

[a] State Key Laboratory of Virology, Wuhan Institute of Virology, Center for Biosafety Mega-Science, Chinese Academy of Sciences, Wuhan, 430071, China

[b] National Laboratory of Biomacromolecules, CAS Center for Excellence in Biomacromolecules, Institute of Biophysics, Chinese Academy of Sciences, Beijing, 100101, China

[c] University of Chinese Academy of Sciences, Beijing, 100049, China

*Corresponding author, email: fli@wh.iov.cn

†Weiwei Zhu and Ti Fang contributed equally to this work.

Materials and Methods

Materials. Fetal bovine serum (FBS), Dulbecco's modified Eagle's medium (DMEM), sodium pyruvate (100 mM), Opti-MEM, Hoechst 33342 (D1306), LysoTracker Red (L7528), and Alexa Fluor 555 NHS ester (A555, A20009) were supplied by Life Technologies (Carlsbad, CA, USA). Penicillin, streptomycin, and Cell Counting Kit-8 (CCK-8, C0038) were purchased from Beyotime Biotechnology (Shanghai, China). Fluorescein isothiocyanate (FITC, F4274); 2',7'-dichlorodihydrofluorescein diacetate (DCFH-DA, D6883); methylene blue (MB, M106894); hydrogen peroxide (H_2O_2, H112520); and iron(II) sulfate heptahydrate ($FeSO_4 \cdot 7H_2O$, F116339) were purchased from Sigma-Aldrich (Saint Louis, MO, USA). Deferoxamine (DFO, D873692) was purchased from Macklin (Shanghai, China). Phorbol 12-myristate 13-acetate (PMA, P167764) was purchased from Aladdin (Shanghai, China). HFF-1 cells were obtained from the Cell Bank of the Chinese Academy of Sciences (Shanghai, China) and cultured in complete medium (DMEM containing 15% FBS, 1 mM sodium pyruvate, 100 U/mL penicillin and 100 μg/mL streptomycin) at 37°C in 5% CO_2.

Plasmid construction, protein preparation and labeling. The genetic modification sites of wtDps were chosen by analyzing its crystal structure (PDB ID: 1QGH) to add the fused peptide on the outer surface of Dps. To add polyhistidine fragments with varied lengths (1-7 histidines) and the spacer peptide (GLNDIFEAQKIEWHE) to the N-terminus of wtDps, eight coding sequences (BDps and H_nBDps, n = 1-7) were constructed with the wtDp gene as the initial template and cloned into the pET32a vector between the *Nde*I and *Xho*I sites. For construction of the expression vector of human ferritin heavy chain (FTH), the coding sequence was cloned into the pET32a vector between the *Nde*I and *Xho*I sites.

The expression and extraction of wtDps, BDps, H_nBDps, and human ferritin heavy chain (FTH) were performed by the same procedure. In particular, the expression was induced by the addition of 1 mM IPTG at 25°C when the cultures reached an OD_{600} of 0.6. Next, cells were harvested after 12 h, suspended and lysed by high-pressure homogenization. After centrifugation at 12,000 ×g for 30 min, the soluble extract was collected, heated at 60°C for 10 min, and centrifuged again at 12,000 ×g for 30 min to recover the supernatant. For purification, wtDps, BDps and H_1BDps in the supernatant were precipitated by ammonium sulfate at 50-80% saturation. The precipitate was suspended in 20 mM Tris-HCl (pH = 7.2), dialyzed overnight to remove residual ammonium sulfate, and further purified by size exclusion chromatography with a Super Index 200 column (GE Healthcare, Madison, WI, USA). In the case of H_nBDps (n = 2-7), the supernatant was applied to a HisTrap HP column (GE Healthcare, Madison, WI, USA) and purified according to the manufacturer's instructions. For purification of FTH, it was precipitated from the supernatants by ammonium sulfate at 20-60% saturation. The precipitate was suspended in phosphate-buffered saline (PBS), which was followed by centrifugation at 12,000 ×g for 30 min. The resulting supernatant was subjected to ultracentrifugation at 50,000 rpm (Ty 70, Beckman, Brea, CA, USA) for 1 h. The precipitate was suspended in PBS. Protein concentration was quantified by SDS-PAGE/densitometry.

To incorporate and mineralize iron oxide nanoparticles in the inner cavity of H_2BDps, a protein solution (0.5 mg/mL H_2BDps in 20 mM MOPS-NaOH, pH 7.0) was bubbled with nitrogen to displace oxygen. After incubation with 1 mM $(NH_4)_2Fe(SO_4)_2$ for 5 min at room temperature, the solution slowly oxidized at room temperature for 20 min in air and was centrifuged at 10,000 ×g for 10 min to remove the precipitate. The collected supernatant was dialyzed against PBS to obtain iron oxide nanoparticles@H_2BDps (IONP@H_2BDps). Iron contents in the inner cavity of H_2BDps (0.7 mg/mL) and IONP@H_2BDps (0.65 mg/mL) were measured by inductively coupled plasma atomic emission spectroscopy (ICP-AES) (IRIS Intrepid II XPS, Thermo, Franklin, MA, USA).

Fluorescence labeling of proteins with A555 or FITC was performed in 100 mM $NaHCO_3$ (pH 8.3) containing 1 mg/mL protein and 70 μg/mL A555 or 150 μg/mL FITC. After incubation for 1 h at room temperature and overnight at 4°C, the modified protein was dialyzed against PBS. Fluorescence of the labeled samples was characterized using an LS55 luminescence spectrometer (PerkinElmer, Waltham, MA, USA).

Transmission electron microscopy (TEM). A protein sample at a concentration of 0.1 mg/mL (20 μL) was dropped on a carbon-coated copper grid. After incubation for 5 min, the solution was removed by filter paper. Then, the grid was stained with 2% phosphotungstate for 5 min. The sample was observed under a Hitachi H7000 TEM equipped with an Olympus MegaView G2 camera. TEM images were processed and analyzed using ImageJ.

Hydrodynamic size and zeta potential measurements. The measurements were performed on a Zetasizer Nano ZS (Malvern Instruments, Malvern, Worcestershire, UK) with automatically optimized parameters. Before hydrodynamic size measurement by dynamic light scattering (DLS), samples were filtered with 0.2-μm syringe filters and then centrifuged at 13,000 rpm for 5 min. Samples were in 1× PBS or 0.2× PBS for hydrodynamic size or zeta potential measurement, respectively. Data were collected by Zetasizer Software Version 6.01.

Cellular uptake analysis. HFF-1 cells were seeded into 12-well plates at 2×10^5/well and cultured overnight. Then, the cells were incubated with 5 μg/mL A555-labeled Dps in Opti-MEM for 4 h and then with complete medium for additional 12 h. Finally, the cells were harvested, suspended in 300 μL ice-cold PBS, and analyzed by flow cytometry (BD LSRFortessa, BD Biosciences, San Jose, CA, USA).

Studies on endocytic pathways and subcellular distribution. For investigation of endocytic pathways, amiloride (1 mM), nystatin (30 μM), and hypertonic sucrose (0.4 M) were used to inhibit micropinocytosis, caveolae/lipid raft-mediated endocytosis, and clathrin-mediated endocytosis, respectively. HFF-1 cells (2×10^5) were seeded in a 35-mm glass-bottomed dish and cultured for 12 h. After further incubation in FBS-free medium for 2 h, the cells were treated with different inhibitors for 1 h at 37°C. Then, the cells were incubated with 5 μg/mL H_nBDps-A555 in Opti-MEM for additional 4 h. After nuclear staining, cell images were captured by a Nikon A1 confocal laser-scanning microscope (Tokyo, Japan) and processed with ImageJ.

For subcellular distribution, HFF-1 cells (2×10^5) were seeded in a 35-mm glass-bottomed dish and cultured for 12 h. After being washed twice with PBS, the cells were incubated with FITC-conjugated H_2BDps (20 μg/mL) in Opti-MEM for 4 h at 37°C. After incubation for additional 20 h with complete medium, the cells were washed with PBS thrice and then fixed with 4% paraformaldehyde for 20 min at room temperature. LysoTracker Red (75 nM) and Hoechst 33342 (5 μg/mL) were added to stain cell lysosomes/endosomes and nuclei, respectively. Fluorescence images were recorded by a Nikon A1 confocal laser-scanning microscope (Tokyo, Japan) and processed with ImageJ. Pearson's coefficients for the colocalization between lysosomes and H_nBDps (n = 2-7) were calculated using Volocity (PerkinElmer, Waltham, MA, USA).

Cytotoxicity analysis. HFF-1 cells were seeded into 96-well plates at 1.0×10^4/well and cultured overnight. After incubation for another 4 h in 100 μL Opti-MEM containing 20 μg/mL Dps, cells were incubated with complete medium for 12 h. Next, 10 μL of CCK-8 solution was added to each well, and the absorbance at 450 nm was measured after 1.5 h by means of an EnSpire 2300 microplate reader (PerkinElmer, Waltham, MA, USA).

Protection of human cells from H_2O_2 challenge. HFF-1 cells were seeded into 24-well plates at 1.0×10^5/well, cultured overnight, and then incubated for another 4 h with Dps at the indicated concentrations in Opti-MEM. Afterwards, the cells were treated with 4 mM H_2O_2 for 12 h and then observed by an Olympus IX73 optical microscope (Tokyo, Japan). Alternatively, after treatment with 4 mM H_2O_2 for 30 min, the cells were incubated with 50 μM DCFH-DA for 30 min. Fluorescence images were captured by an IX73 microscope to detect intracellular ROS. Cell viability was determined by CCK-8.

In vitro inhibitory effect of Dps on the Fenton reaction. A solution of methylene blue (MB) (31.3 μM in ddH_2O) containing 35.8 μM $FeSO_4$ and 441 μM H_2O_2 was mixed at the indicated concentrations of Dps for 20 min at room temperature, and the developed absorbance was measured at 665 nm (A_i) by an EnSpire 2300 microplate reader. The absorbance at 665 nm of MB solution (A_o) and MB solution with $FeSO_4$ and H_2O_2 (A_c) were used as blanks. The apparent inhibition rate was calculated as $((A_i\text{-}A_c)/(A_o\text{-}A_c)) \times 100\%$.[1]

Anti-inflammation of Dps in vivo. SPF (Specific Pathogen Free) female ICR mice (6 weeks) purchased from Beijing Wei-tong Li-hua Experimental Animal Technology Co. Ltd (Beijing, China) were used to establish a PMA-induced inflammation model as previously described.[2] Next, the mice were subcutaneously injected with Dps proteins at a dose of 15 mg/kg 5 h after PMA induction. After 1.5 h, 50 μL of DCFH-DA (1 mM) was subcutaneously injected. After incubation for 0.5 h, the ROS levels of mice were recorded after hair removal by a PerkinElmer *In vivo* Imaging System (Ex: 488 nm; Em: 520 nm). Alternatively, the right ears were isolated and fixed in 4% PFA after washing with PBS. Then, the tissues were sectioned at a thickness of 5 μm, stained with hematoxylin and eosin (H&E), and imaged by a Pannoramic MIDI system (3DHISTECH, Budapest, Hungary).

Supplementary Results and Discussion

Members of the ferritin-like superfamily are abundantly found in all life forms as iron storage proteins.[3] Although human ferritins are cytoprotective antioxidants as they mineralize iron,[4] their mineralization mechanism is different from that of Dps. Specifically, human ferritins use O_2 as the oxidant to oxidize and mineralize Fe^{2+}, whereas Dps exhibits a higher reactivity with H_2O_2. The rate of Fe^{2+} oxidation by H_2O_2 in Dps is 1,000-fold faster than that by O_2, and the rate of Fe^{2+} oxidation by O_2 in Dps is much slower than that in human ferritins.[5] Therefore, the antioxidant activity of Dps is not impaired by ubiquitous O_2, unlike human ferritins and is only activated in the presence of H_2O_2. As Dps eliminates both Fe^{2+} and H_2O_2, it should be advantageous over human ferritins in preventing oxidative damage from the Fenton reaction.

To investigate the difference, the antioxidant activity of FTH was compared to H_2BDps. The cage-like morphology of FTH was confirmed by TEM after expression and purification (Fig. S7). Cell internalization studies confirmed that FTH and H_2BDps exhibited similar uptake efficiencies by HFF-1 cells under equivalent conditions (Fig. S8). Moreover, previous studies have shown that FTH is internalized through clathrin-mediated endocytosis,[6] which is similar to H_2BDps. When challenged with H_2O_2, cells treated with H_2BDps demonstrated a normal spindle shape, whereas cells pretreated with FTH demonstrated an apoptotic morphology (Fig. S9a). The viability of cells pretreated with FTH was reduced to less than 20%, which is similar to that of the PBS-pretreated cells (Fig. S9b). Brightfield microscopy analysis and the CCK-8 assay consistently demonstrated that FTH did not protect HFF-1 cells from oxidative damage. Clearly, Dps is a unique antioxidant for human cells because it sequesters Fe^{2+} only in the response of H_2O_2, which is an advantage over human ferritins.

Desferrioxamine (DFO), an FDA-approved, representative antioxidant, takes effect by chelating iron ions to inhibit the Fenton reaction.[7] Therefore, the antioxidant activity of H_2BDps was also compared with DFO. As shown in Fig. S9a,b, when HFF-1 cells were pretreated with DFO at gradient concentrations (0.03, 0.33, and 3.33 mg/mL) and challenged with 4 mM H_2O_2, the cells pretreated with DFO at lower concentrations shrank remarkably and exhibited less than 30% viability. Even at the highest tested concentration of DFO (3.33 mg/mL), the cell viability was only 59.7%, which was lower than that of the 20 μg/mL H_2BDps-pretreated group (86.3%). The significantly lower efficacy of DFO may be due to poor cellular uptake and cytotoxicity at high concentrations.[8] The comparison demonstrated that H_2BDps performs much better than the classical iron chelator DFO.

Supplementary Figures

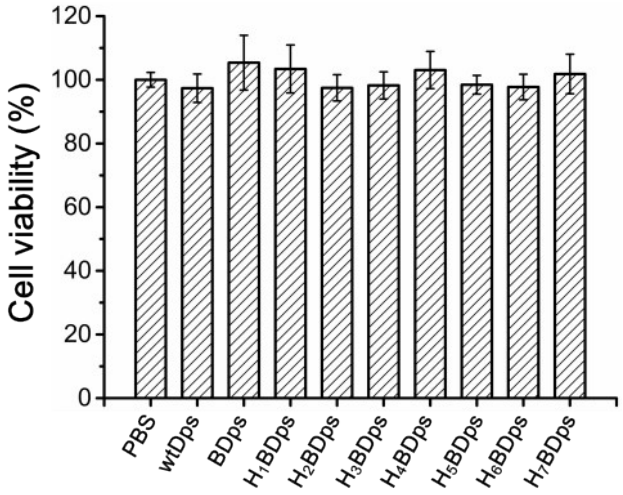

Fig. S1 Viability of HFF-1 cells incubated with different H_nBDps constructs (20 μg/mL) analyzed using the CCK-8 assay. Data are means ± SD of triplicate experiments.

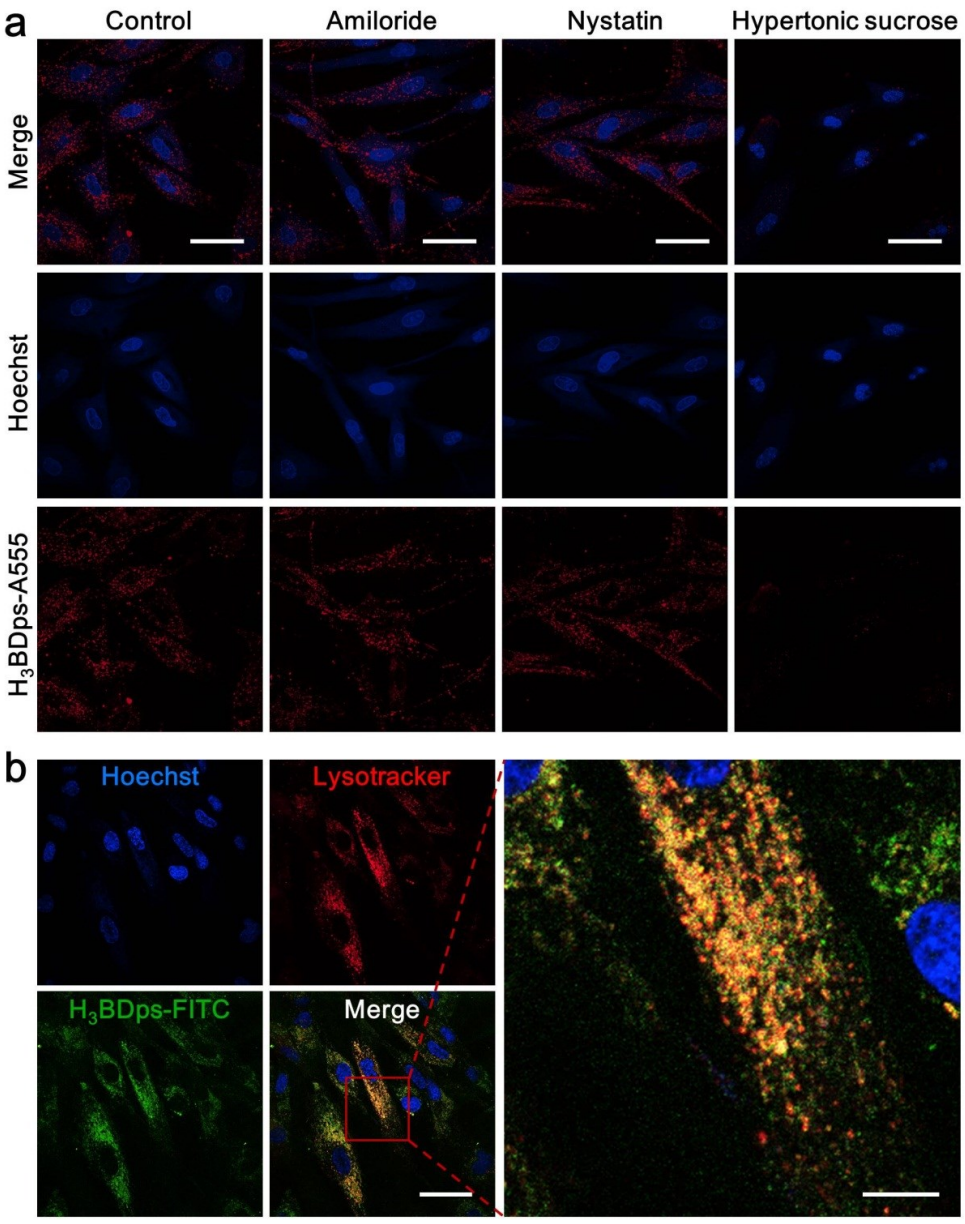

Fig. S2 Endocytic mechanism of H_3BDps. (**a**) Confocal microscopy imaging of the endocytic pathway of H_3BDps. HFF-1 cells were treated with different inhibitors for 1 h at 37°C. Nontreated cells were used as controls. The cells were incubated for 4 h with Opti-MEM containing A555-labeled H_3BDps (H_3BDps-A555; 5 μg/mL) and then imaged. Only hypertonic sucrose inhibited the internalization of H_3BDps. (**b**) Confocal microscopy imaging of the subcellular distribution of H_3BDps. HFF-1 cells were incubated with FITC-conjugated H_3BDps (5 μg/mL) for 4 h at 37°C and then with complete medium for 20 h. The cells were fixed, stained with LysoTracker Red (75 nM) and Hoechst 33342 (5 μg/mL) for 20 min, and then imaged. Here, H_3BDps was labeled by FITC instead of A555 to avoid cross-talk with LysoTracker Red. H_3BDps was colocalized with endosomes/lysosomes with a Pearson's correlation coefficient of 0.69 ± 0.02. Scale bars = 50 μm or 10 μm (zoom-in).

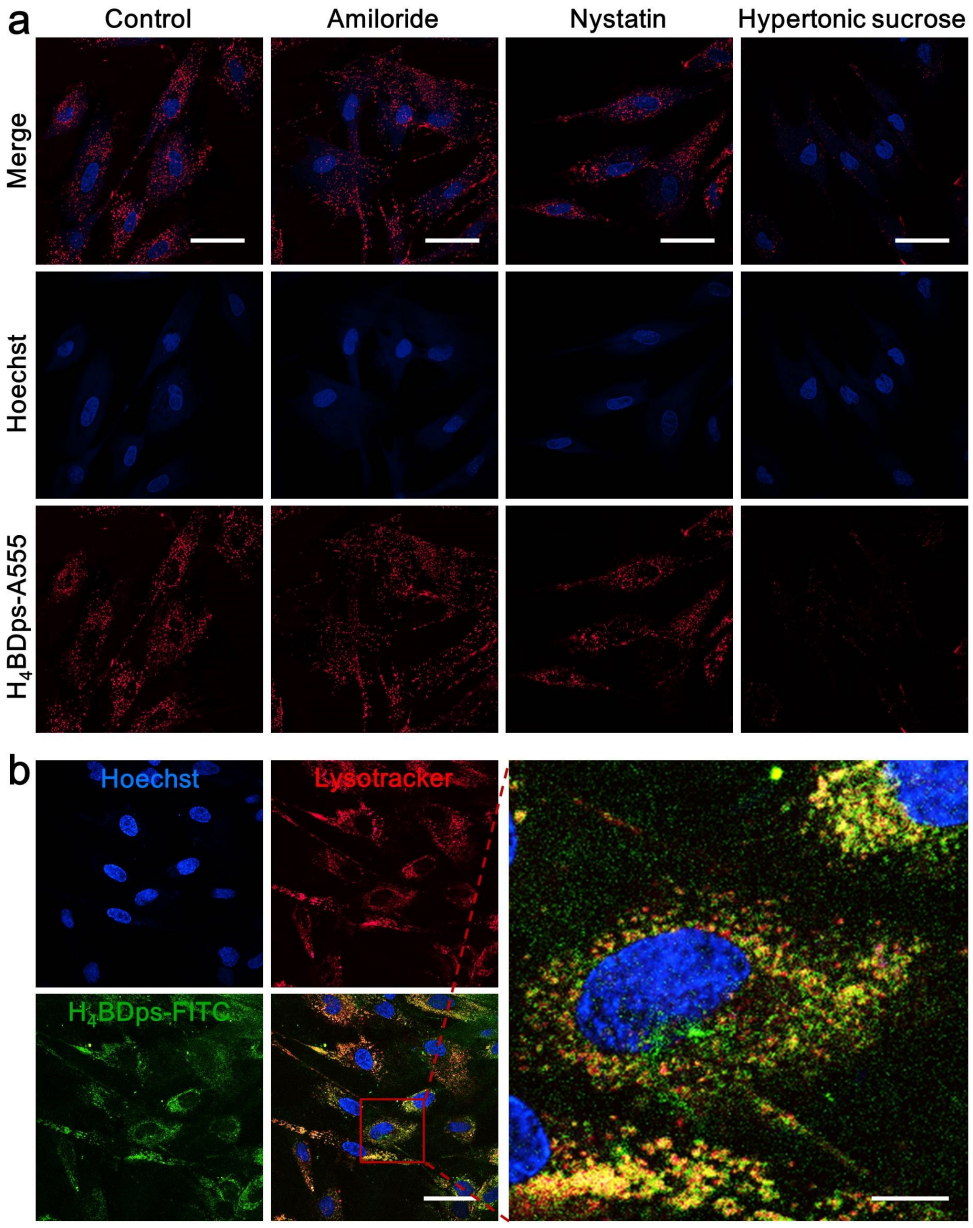

Fig. S3 Endocytic mechanism of H_4BDps. (**a**) Confocal microscopy imaging of the endocytic pathway of H_4BDps. HFF-1 cells were treated with different inhibitors for 1 h at 37°C. Nontreated cells were used as controls. The cells were incubated for 4 h with Opti-MEM containing A555-labeled H_4BDps (H_4BDps-A555; 5 μg/mL) and then imaged. Only hypertonic sucrose inhibited the internalization of H_4BDps. (**b**) Confocal microscopy imaging of the subcellular distribution of H_4BDps. HFF-1 cells were incubated with FITC-conjugated H_4BDps (5 μg/mL) for 4 h at 37°C and then with complete medium for 20 h. The cells were fixed, stained with LysoTracker Red (75 nM) and Hoechst 33342 (5 μg/mL) for 20 min, and then imaged. Here H_4BDps was labeled by FITC, instead of A555 to avoid crosstalk with LysoTracker Red. H_4BDps was colocalized with endosomes/lysosomes with a Pearson's correlation coefficient of 0.64 ± 0.08. Scale bars = 50 μm or 10 μm (zoom-in).

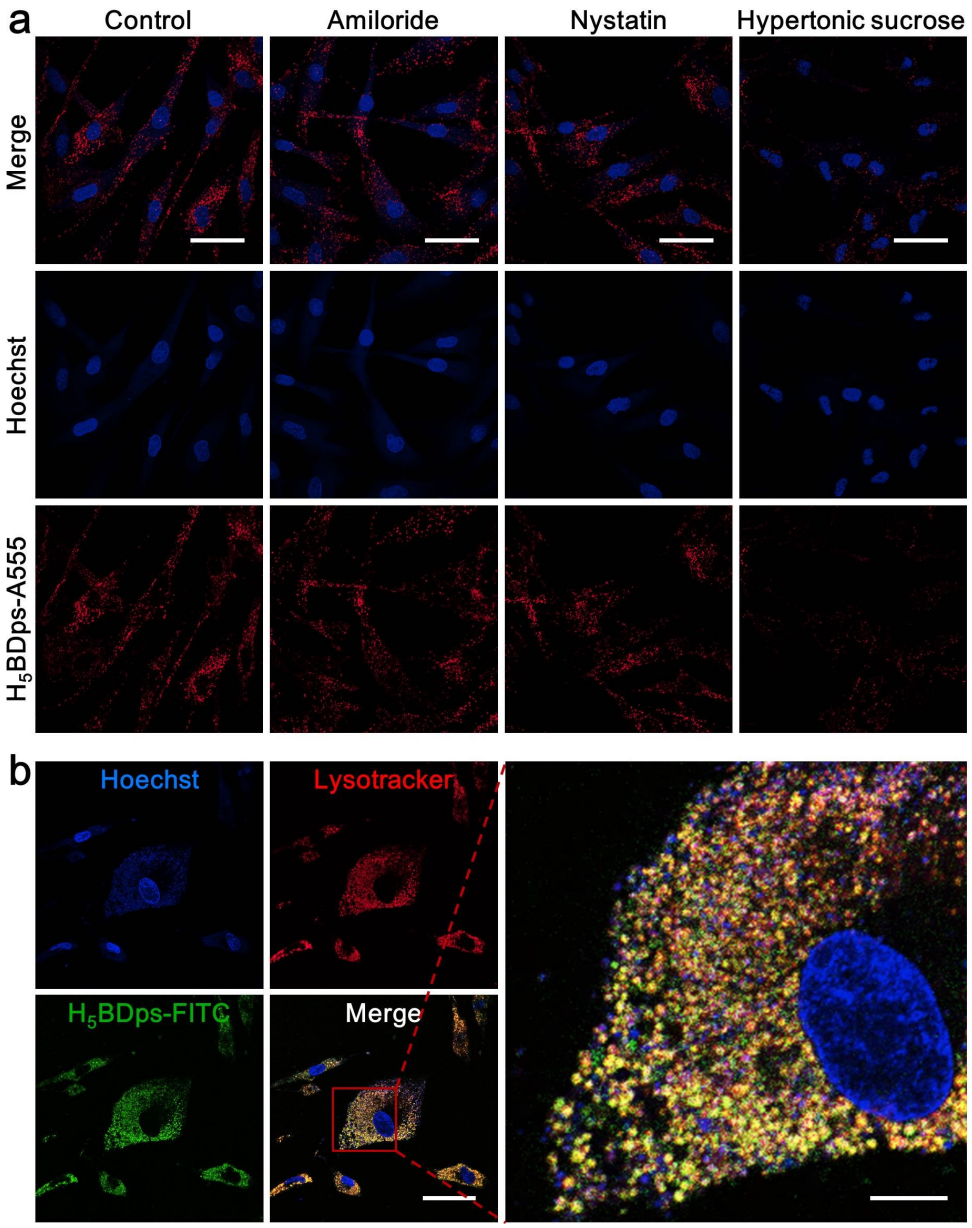

Fig. S4 Endocytic mechanism of H_5BDps. (**a**) Confocal microscopy imaging of the endocytic pathway of H_5BDps. HFF-1 cells were treated with different inhibitors for 1 h at 37°C. Nontreated cells were used as controls. The cells were incubated for 4 h with Opti-MEM containing A555-labeled H_5BDps (H_5BDps-A555; 5 μg/mL) and then imaged. Only hypertonic sucrose inhibited the internalization of H_5BDps. (**b**) Confocal microscopy imaging of the subcellular distribution of H_5BDps. HFF-1 cells were incubated with FITC-conjugated H_5BDps (5 μg/mL) for 4 h at 37°C and then with complete medium for 20 h. The cells were fixed, stained with LysoTracker Red (75 nM) and Hoechst 33342 (5 μg/mL) for 20 min, and then imaged. Here H_5BDps was labeled by FITC, instead of A555 to avoid crosstalk with LysoTracker Red. H_5BDps was colocalized with endosomes/lysosomes with a Pearson's correlation coefficient of 0.66 ± 0.05. Scale bars = 50 μm or 10 μm (zoom-in).

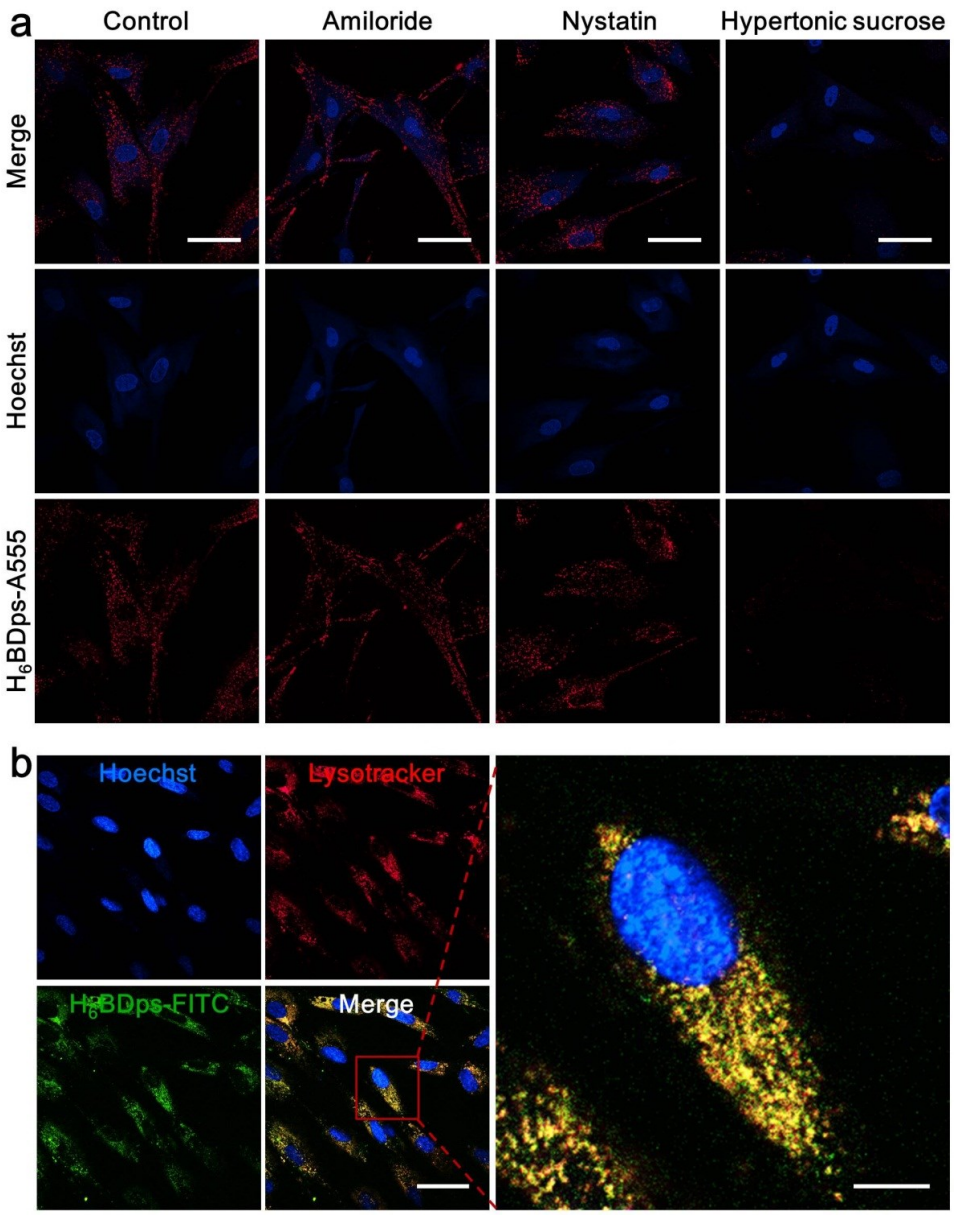

Fig. S5 Endocytic mechanism of H_6BDps. (**a**) Confocal microscopy imaging of the endocytic pathway of H_6BDps. HFF-1 cells were treated with different inhibitors for 1 h at 37°C. Nontreated cells were used as controls. The cells were incubated for 4 h with Opti-MEM containing A555-labeled H_6BDps (H_6BDps-A555; 5 μg/mL) and then imaged. Only hypertonic sucrose inhibited the internalization of H_6BDps. (**b**) Confocal microscopy imaging of the subcellular distribution of H_6BDps. HFF-1 cells were incubated with FITC-conjugated H_6BDps (5 μg/mL) for 4 h at 37°C and then with complete medium for 20 h. The cells were fixed, stained with LysoTracker Red (75 nM) and Hoechst 33342 (5 μg/mL) for 20 min, and then imaged. Here H_6BDps was labeled by FITC, instead of A555 to avoid crosstalk with LysoTracker Red. H_6BDps was colocalized with endosomes/lysosomes with a Pearson's correlation coefficient of 0.66 ± 0.07. Scale bars = 50 μm or 10 μm (zoom-in).

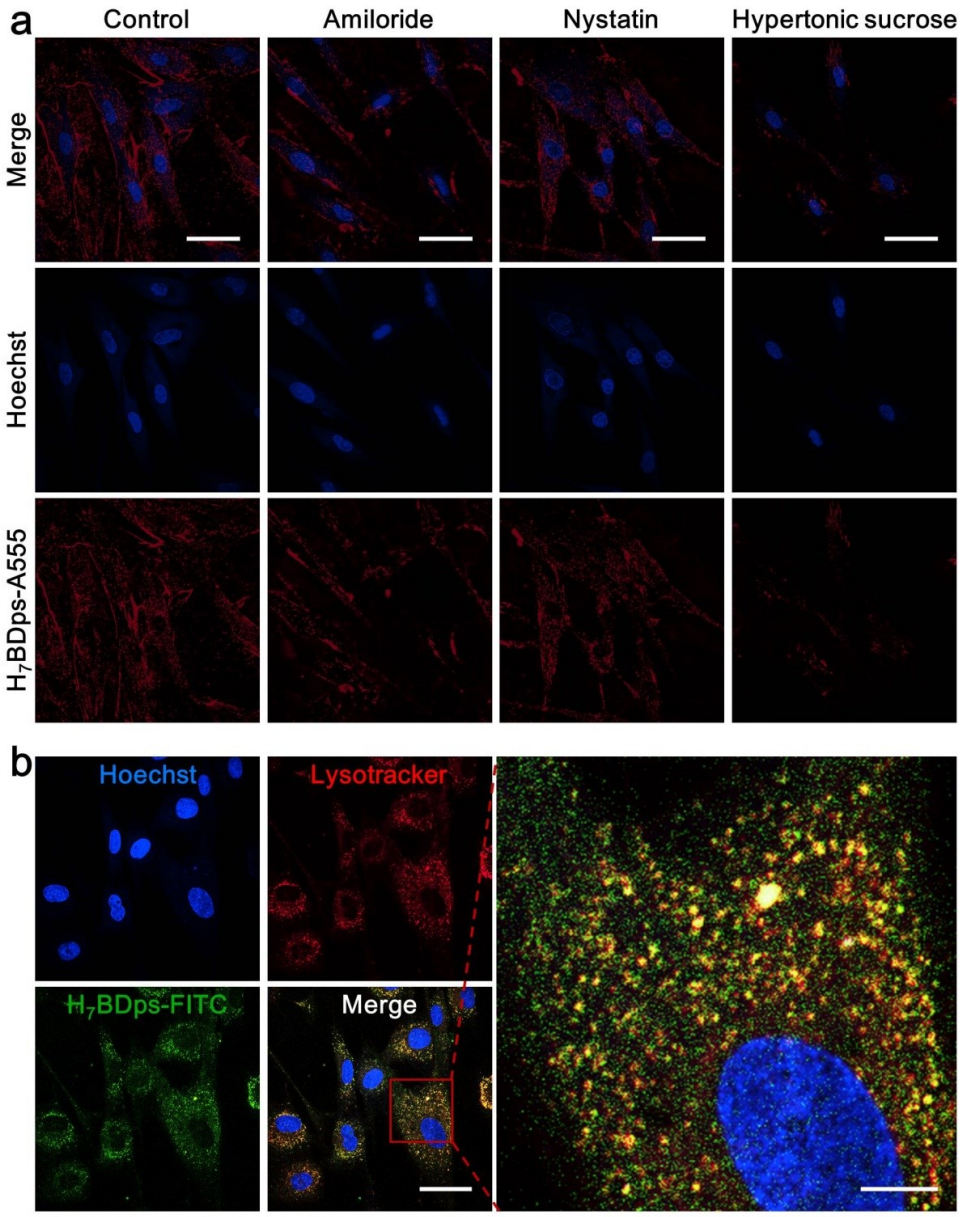

Fig. S6 Endocytic mechanism of H_7BDps. (**a**) Confocal microscopy imaging of the endocytic pathway of H_7BDps. HFF-1 cells were treated with different inhibitors for 1 h at 37°C. Non-treated cells were used as controls. The cells were incubated for 4 h with Opti-MEM containing A555-labeled H_7BDps (H_7BDps-A555; 5 μg/mL) and then imaged. Only hypertonic sucrose inhibited the internalization of H_7BDps. (**b**) Confocal microscopy imaging of the subcellular distribution of H_7BDps. HFF-1 cells were incubated with FITC-conjugated H_7BDps (5 μg/mL) for 4 h at 37°C and then with complete medium for 20 h. The cells were fixed, stained with LysoTracker Red (75 nM) and Hoechst 33342 (5 μg/mL) for 20 min, and then imaged. Here H_7BDps was labeled by FITC, instead of A555 to avoid crosstalk with LysoTracker Red. H_7BDps was colocalized with endosomes/lysosomes with a Pearson's correlation coefficient of 0.59 ± 0.07. Scale bars = 50 μm or 10 μm (zoom-in).

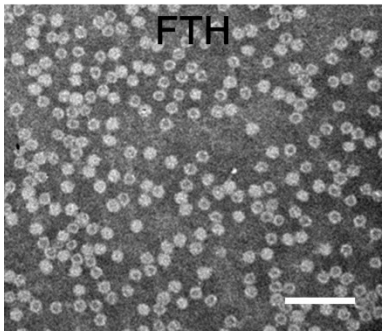

Fig. S7 Negative-staining TEM image of FTH. Scale bar = 50 nm.

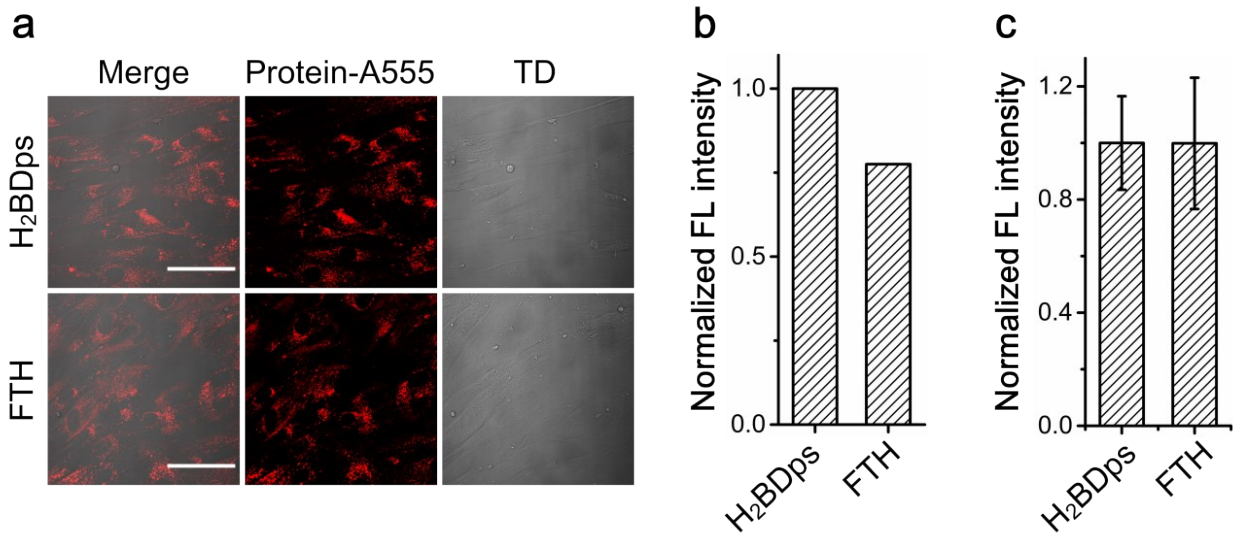

Fig. S8 Comparison of cellular uptake between H_2BDps and FTH. (**a**) After incubation with 81.9 nM (based on protein cages) A555-modified H_2BDps or FTH in Opti-MEM for 4 h, HFF-1 cells were cultured in complete medium for additional 12 h and then imaged. Confocal images reveal that the two types of protein cages were internalized by HFF-1 cells. Scale bars = 50 μm. (**b**) Normalized fluorescence (FL) intensity of H_2BDps and FTH labeled with A555. Both samples were diluted to a protein concentration of 41 nM and excited at 550 nm with the fluorescence intensity at 580 nm recorded on a luminescence spectrometer. (**c**) Quantitative analysis of the cellular uptake of H_2BDps and FTH via Volocity software indicated that the cellular uptake efficiencies of H_2BDps and FTH were similar. The fluorescence intensities were standardized based on the normalized fluorescence intensity of H_2BDps and FTH in (b) and normalized to that of cells incubated with H_2BDps. Data are means ± SD of triplicate experiments.

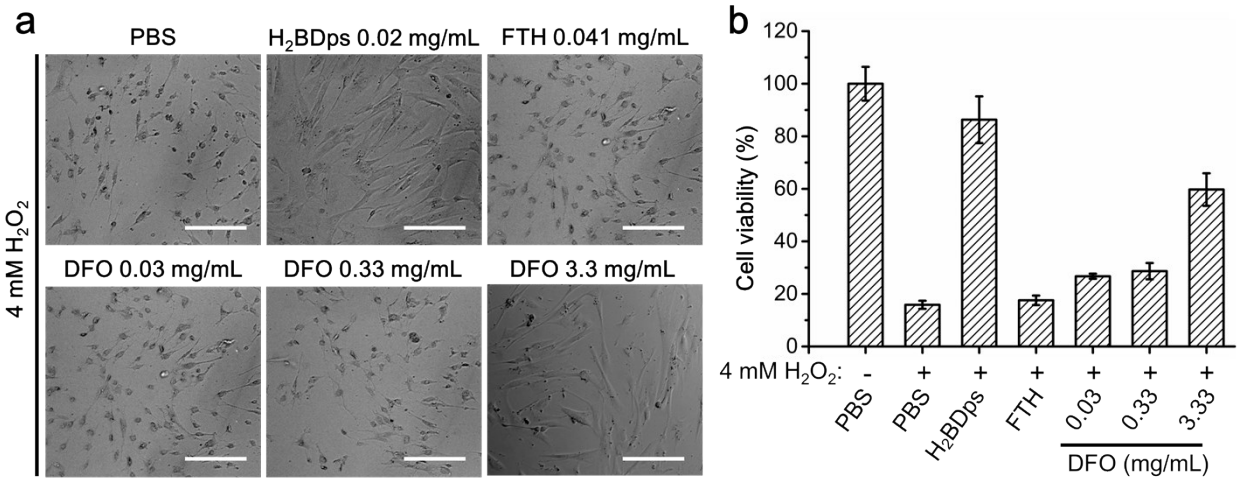

Fig. S9 Comparison of antioxidant effects among H_2BDps, FTH, and DFO in cultured cells. HFF-1 cells were incubated with 20 μg/mL H_2BDps, 41 μg/mL FTH, or 0.03-3.33 mg/mL DFO for 4 h and then treated with 4 mM H_2O_2 for 12 h followed by microscopic imaging (**a**) and CCK-8 assay (**b**). The molar concentrations of H_2BDps and FTH used were equivalent (81.9 nM of protein cages), and that of DFO ranged from 0.05 to 5 mM (corresponding to 0.03-3.33 mg/mL). Scale bars = 200 μm. Data are means ± SD of triplicate experiments.

Fig. S10 Image of the mouse with an inflamed right ear induced by PMA.

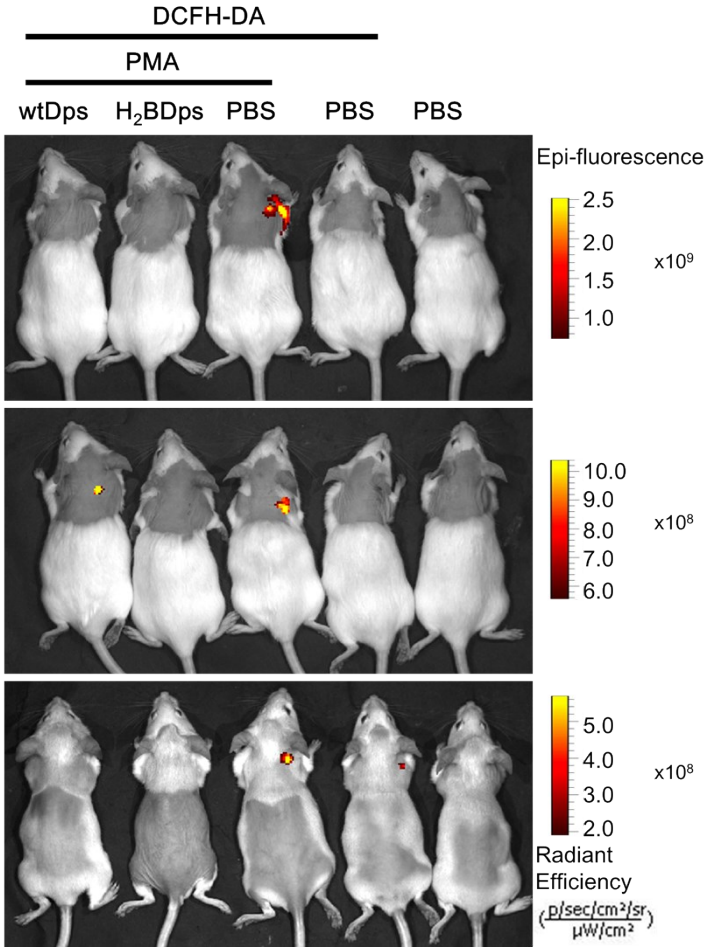

Fig. S11 Fluorescence images of mice with PMA-induced ear inflammation after treatment with 15 mg/kg H_2BDps or wtDps through subcutaneous injection.

REFERENCES

1 K. Dutta, S. Mukhopadhyay, S. Bhattacharjee and B. Chaudhuri, *J. Hazard.Mater.*, 2001, **84**, 57-71.

2 J. Yao, Y. Cheng, M. Zhou, S. Zhao, S. Lin, X. Wang, J. Wu, S. Li and H. Wei, *Chem. Sci.*, 2018, **9**, 2927-2933.

3 G. Jutz, P. van Rijn, B. Santos Miranda and A. Böker, *Chem. Rev.*, 2015, **115**, 1653-1701.

4 G. Balla, H. S. Jacob, J. Balla, M. Rosenberg, K. Nath, F. Apple, J. W. Eaton and G. M. Vercellotti, *J. Biol. Chem.*, 1992, **267**, 18148-18153.

5 M. Su, S. Cavallo, S. Stefanini, E. Chiancone and N. D. Chasteen, *Biochemistry*, 2005, **44**, 5572-5578.

6 S. W. Hulet, S. O. Heyliger, S. Powers and J. R. Connor, *J. Neurosci.Res.*, 2000, **61**, 52-60.

7. P. Holden and L. S. Nair, *Tissue Eng. Part B Rev.*, 2019, **25**, 461-470.

8. B. Halliwell, *Free Radic.Biol. Med.*, 1989, **7**, 645-651.